

Phase separation of binary fluids in porous media: Asymmetries in pore geometry and fluid composition

Zhengping Zhang and Amitabha Chakrabarti

Department of Physics, Kansas State University, Manhattan, Kansas 66506

(Received 16 March 1995)

Phase separation of a binary Lennard-Jones fluid confined in a variety of two-dimensional pores is studied using molecular dynamics simulations. We consider a simple strip pore, an uneven single pore, and a junction made out of two pores. We have studied dynamics of phase separation for both critical and off-critical composition of the binary fluid. We find the existence of long-lived metastable states in the presence of asymmetries both in the geometry and the composition of the fluid. The results are compared with theoretical predictions and with experimental observations.

PACS number(s): 68.45.Gd, 64.60.-i, 47.55.Mh

I. INTRODUCTION

Binary fluid mixtures inside porous media have been extensively studied recently by both experimentalists and theoretists due to their rich phase behavior and potential materials applications [1–7]. In contrast to the macroscopic phase separation that characterizes bulk mixtures inside the miscibility gap, the general feature found in liquid mixtures inside porous media is metastability and slow kinetics of phase separation. For example, during the phase separation of binary fluids imbibed in Vycor glasses [1,2], the two phases do not separate completely even deep inside the coexistence region; instead, they form many long-lived microdomains, rich in one phase or the other. Although theoretical understanding of phase separation in these systems is far from complete, two different interpretations have been introduced. In one interpretation, the metastability and the slow dynamics are explained in terms of the conserved dynamics of a random field Ising model [8], which is obtained from a coarse-grained description of the phase separation process in the presence of the random convolutions of the pore surface [8]. It has been criticized, however, that such a mapping onto the random field Ising model is not applicable for low-porosity media such as Vycor glasses [3,4]. The second interpretation is to relate the metastability to the geometric confinement of the binary mixture inside a pore [3]. Such a single-pore model without any randomness has been used as a model system [3,4,6,7] to understand various effects observed in experiments with Vycor glasses [1,2,9]. In the original work introducing the single-pore model [3], it was argued that the wetting behavior of the fluids at pore surfaces plays a major role in preventing macroscopic phase separation. In the same work the wetting phase diagram for a single-pore model with a long-ranged wetting potential is derived using a mean-field approach [3]. Except at low surface fields, the wetting phase diagram is qualitatively verified by Monte Carlo simulation studies of an Ising model confined in a pore [4], in which only a short-range interaction is involved. A more quantitative estimate of the breakdown

of the power-law growth of domains (which is seen in bulk mixtures) is obtained using Langevin simulations [6]. The recent molecular-dynamics simulation study [7] provides strong evidence to show that long-lived metastable states exist even in the presence of hydrodynamic modes. Although these numerical work employ different range of interactions and different dynamical evolution process, they all start with a binary liquid mixture confined in a single small pore and find that it is the confinement in a small pore that leads to the slowing down of the domain growth process. However, the molecular-dynamics study indicates, as the Monte Carlo simulation studies also do, that the details of the mean-field calculations may not be valid in more realistic situations.

In a true porous medium like Vycor, there are pore junctions and variations in the pore radius. Effects of these geometrical asymmetries on the phase separation process is the main concern of this paper. Recent studies have addressed this question by carrying out simulations in a Vycor-like geometry in two dimensions. It has been found that the kinetics of domain growth dramatically slows down as the average size of the domains become comparable to the average radius of the pores [10–12]. Although the results of the simulations support the applicability of the single-pore model in a general sense, the important role played by the pore junctions on the domain formation has not been studied in detail in these previous simulations. With an eye to this direction, we carry out molecular-dynamics simulations of a model two-dimensional binary fluid confined in pores that have asymmetries in their geometrical shape. We also consider asymmetries in the composition of the fluid (off-critical composition of the fluid mixture). The single-pore model allows for various long-lived metastable configurations (called “plugs” and “capsules”) whose stability depends on the temperature and the strength of the interaction of the pore surface with one of the components of the mixture. However, at low temperatures and for weak surface interaction, the plug configuration is always expected. In this paper, we study the stability of this plug phase in the

presence of asymmetries both in geometry and in composition of the binary fluid mixture.

In Sec. II we define the models and describe the computational method used in the paper. The results are presented in Sec. III, and the paper is concluded in Sec. IV by a discussion of the results in relation to previous theoretical work and experiments.

II. MODEL AND COMPUTATIONAL METHODS

Our model system consists of two species A and B confined in two-dimensional pore junctions and single pores with variations in the pore radius. The molecules move in the two-dimensional confined region and interact via Lennard-Jones potentials. The potential energies of the molecules are of forms

$$U_{AA}(r) = U_{BB}(r) = 4\epsilon[(\sigma/r)^{12} - (\sigma/r)^6], \quad (1)$$

$$U_{AB}(r) = 4\epsilon[(\sigma/r)^{12}] \quad (2)$$

for the molecules of the same species and different species, respectively. The parameters ϵ and σ are used as units of energy and distance in our simulations.

There are three types of simplified pores we study in the paper: a simple strip pore, an uneven single pore, and a junction of pores. The first one is made of a single narrow strip, the uneven single pore consists of a rhombus connected to the two ends of a strip pore, and the junction consists of two strip pores that cross and are perpendicular to each other. The periodic boundary condition is applied in the direction of their long symmetric axes.

We study the two-dimensional fluid using the molecular-dynamics simulation method. The algorithm we used in our simulations is the so-called ‘‘velocity Verlet’’ algorithm, which has an advantage of updating positions, velocities, and accelerations all at the same time t [13]. The velocity Verlet algorithm takes the form

$$\begin{aligned} \mathbf{r}(t + \delta t) &= \mathbf{r}(t) + \delta t \mathbf{v}(t) + \frac{1}{2} \delta t^2 \mathbf{a}(t), \\ \mathbf{v}(t + \delta t) &= \mathbf{v}(t) + \frac{1}{2} \delta t [\mathbf{a}(t) + \mathbf{a}(t + \delta t)], \end{aligned} \quad (3)$$

where \mathbf{r} , \mathbf{v} , and \mathbf{a} are positions, velocities, and accelerations, respectively. The accelerations $\mathbf{a}(t)$ are calculated from the potentials described in Eqs. (1) and (2) for given positions $\mathbf{r}(t)$. The potentials are truncated at 2.5σ to save computer processing unit times for numerically solving the equations of motion.

The simulations are carried out at constant volume (area) with a reduced fluid number density $\rho^* = N\sigma^2/V \approx 0.8$, where N is the total number of molecules in the system of volume (area) V . A hexagonal lattice of molecules of one species was used to generate the initial configuration with the same number density. The initial velocities of molecules were generated from the Maxwell-Boltzmann velocity distribution at a very high temperature. We then let the system melt at this high temperature until the potential energy is equilibrated and a large value for the mean squared displacements of molecules from their initial lattice positions are observed. A quench at a reduced temperature $T^* = 1.4$, in units of ϵ , below the bulk consolute temperature is performed after

the initial equilibration [14,15]. We do not know accurately the consolute temperature in the two-dimensional system. However, based on the fact that we observed clear phase separation processes at $T^* = 1.4$ in a bulk two-dimensional (2D) mixture, we believe this temperature is well below the consolute temperature of the binary mixture system. However, we observed strong fluctuations in the 2D simulation data, in contrast to the corresponding 3D simulation ones, which indicates that a quench at $T^* = 1.4$ in 2D is shallower than that in 3D simulations [7]. The system is then evolved isothermally by rescaling velocities of the molecules every time step by a factor of $(T^*/\mathcal{K})^{1/2}$, where \mathcal{K} is the current kinetic energy per molecule. Being rescaled, the current kinetic energy per molecule then is the same as given by the desired thermodynamic temperature T^* . After the system reaches equilibrium at the temperature T^* , the molecules are labeled A and B randomly. Then a phase separation starts because of strong repulsive interactions between the different species as described in Eq. (2) [14,15]. The process of phase separation is studied by monitoring the decay of the total interaction potential energy between the two species and the configurations of molecular positions.

Infinite hard wall interaction is introduced for all of the situations considered in the paper. If a molecule with a velocity \mathbf{v} collides on the wall at the position \mathbf{r} where the normal to the wall is $\mathbf{n}(\mathbf{r})$, it will bounce at the velocity of $\mathbf{v}' = \mathbf{v} - 2(\mathbf{v}, \mathbf{n})\mathbf{n}$, where (\mathbf{v}, \mathbf{n}) refers to the scalar product of the two vectors. An integration time step of $\delta t = 0.001\tau$ is used in most of our simulations. Test runs using other values of δt showed that the chosen value is small enough for our purpose. Time is measured in units of $\tau = (m\sigma^2/\epsilon)^{1/2}$, where m is the mass of the fluid molecule.

III. RESULTS

We shall mainly concentrate on the symmetric case (equal area fraction of species A and B) and only present some selected results for the nonsymmetric (off-critical) case for the purpose of comparison. After the initial equilibration at $T^* = 1.4$, quenches start with the configurations in which the species A and B were well mixed. An instability against infinitesimal long-wavelength fluctuations in the ordering leads to the formation of small domains, rich in species either A or B , and their subsequent temporal growth. The growth follows a simple and generic form, $R(t) \sim t^\alpha$, where $R(t)$ corresponds to the average size of the ordering domains, and the growth exponent α is believed to be characteristic of the dynamical universality class to which the system belongs, which depends on few general constraints such as conservation laws [16] and the presence or the absence of hydrodynamic modes [17]. Dynamical scaling is a consequence of the presence of one dominant length scale in the system. The growth exponent for a binary alloy is $\frac{1}{3}$, characteristic of the bulk diffusion of molecules between the ordering domains [18,19]. However, in the presence of hydrodynamics modes, the growth exponent for binary fluid mixtures in three dimensions crosses over

from $\frac{1}{3}$ to unit at late times [17,20]. In two dimensions the value of the late-time (hydrodynamic) growth exponent seems to be less than unity ($\approx \frac{2}{3}$) [21]. To monitor the domain growth, the repulsive potential energy between two species, $U_{AB}(t)$ in Eq. (2), is computed after the quenches. It measures the reduction of interfaces between the species A and B , and, therefore, is a good indicator of the phase separation process. The domain growth exponent in the late stage α can be estimated from the data for $U_{AB}(t)$ in combination with the relation of $U_{AB} \sim t^{-\alpha}$ [14,15]. We believe that the growth exponent obtained in this way is an effective exponent since its value is dependent on the size of the pores under study. However, the exponent is still useful for understanding the dynamics of domain growth of the fluid mixtures confined in finite geometries.

In Fig. 1 we present the configuration snapshots, taken at several instants, of the symmetric species confined within a simple strip pore of radius $R = 5.6\sigma$ and length $L = 112\sigma$. The system starts to form a plug configuration at $t \sim 100\tau$, at which time there are rough interfaces between the different species. The interfaces then move due to the diffusion of molecules driven by the surface tension and the domain size grows slowly. At a later time, $t \sim 800\tau$, the interfaces become sharper and the plug configuration becomes stable up to a very late time, which we have checked in our simulations until $t \sim 2000\tau$. The diffusion process can be observed even clearly in the case of the off-critical composition of the fluid mixture. We filled up the same strip pore with 80% A and 20% B and then did the same quench as that in the previous case. In Fig. 2 we show the configuration snapshots of the off-critical mixture at several instants. Small domains of the species B are formed in the vicinity of the pore surface in order to reduce the interface with the species A . Then the small domains move along the pore surface and grow through combining with each other. When the domain size is compatible to the pore size, a plug is formed. As soon as the plug is formed, the

50-50 composition

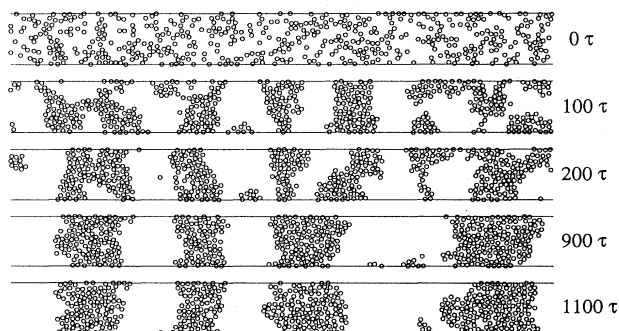


FIG. 1. The configuration snapshots of 50-50 composition mixtures confined in a simple strip pore of radius $R = 5.6\sigma$ and length $L = 112\sigma$ at $t = 0, 100\tau, 200\tau, 900\tau$, and 1100τ after a quench at $T^* = 1.4$. The reduced number density of the mixture is $\rho^* \approx 0.8$. One of the two species is shown as \circ , the other one is not shown for clarity.

80-20 composition

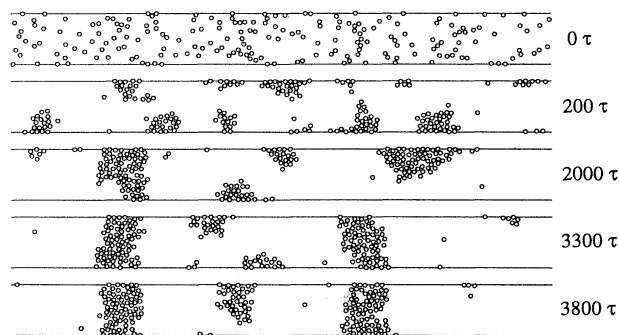


FIG. 2. The configuration snapshots of a 80-20 fluid mixture confined in the same strip pore as shown in Fig. 1 at $t = 0, 200\tau, 2000\tau, 3000\tau$, and 3800τ after a quench at $T^* = 1.4$. The reduced number density of the mixture is $\rho^* \approx 0.8$. The minority component is shown as \circ , the other one is not shown for clarity.

domain hardly moves and its shape becomes stable. However, it takes a much longer time to have a plug phase in this case than in the previous one because of a low density of the species B . In this case, we observed stable plugs until $t \sim 4000\tau$. In Fig. 3, we show a log-log plot of the repulsive potential energy between different species as a function of time for both cases. The energy for the symmetric case is higher, on average, than that for the asymmetric case, as one expects. The effective growth exponents estimated from the repulsive potential energies (computed until stable plugs are formed) are very close to each other in these two cases: 0.32 ± 0.04 for the symmetric case and 0.29 ± 0.04 for the off-critical case, respectively. It seems that the domain growth exponent in these cases is given by the purely diffusive growth exponent of $\frac{1}{3}$.

Figure 4 shows configuration snapshots during the evolution of the symmetric mixture system confined within an uneven strip pore. The length of the pore is $L = 112\sigma$. The largest and smallest radii of the pore are

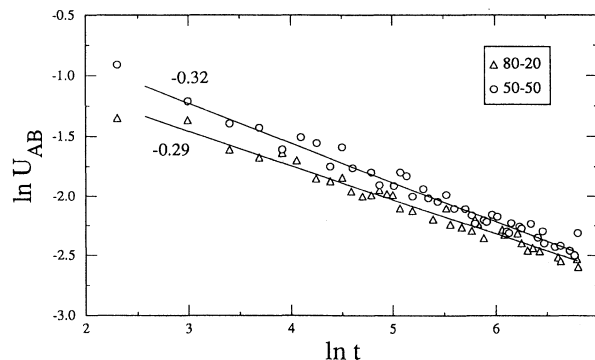


FIG. 3. Log-log plot of the repulsive potential energies between the two different species vs time for the two fluid mixtures shown in Figs. 1 and 2. The solid lines with the slopes as shown are obtained as the best fits to the data.

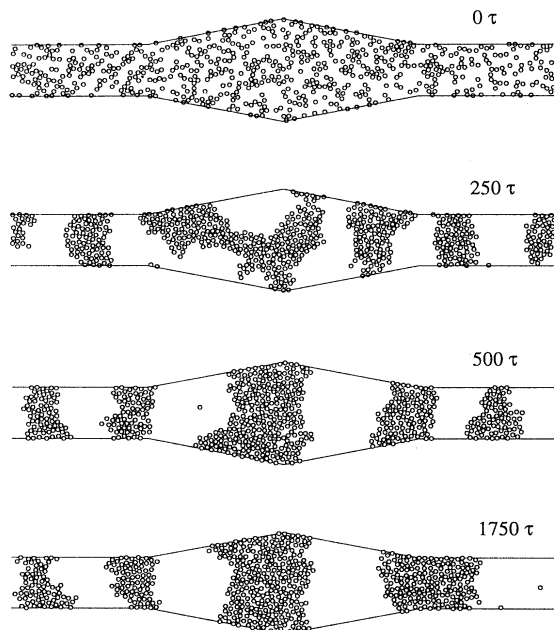


FIG. 4. The configuration snapshots of a 50-50 composition mixture confined in an uneven strip pore of $R_{\min} = 5.6\sigma$, $R_{\max} = 11.2\sigma$, and $L = 112\sigma$ at $t = 0, 250\tau, 500\tau$, and 1750τ after a quench at $T^* = 1.4$. The reduced number density of the mixture is $\rho^* \approx 0.8$. The tilt angle in the wider section is $\theta = 11.3^\circ$. One of the two species is shown as \circ , the other one is not shown for clarity.

$R_{\max} = 11.2\sigma$ and $R_{\min} = 5.6\sigma$, respectively. The tilt angle of the walls of the uneven section is $\theta = 11.3^\circ$. One can see in Fig. 4 that the domain sizes are obviously different in different parts of the pore and they are determined approximately by local pore sizes. The effective growth exponent for this case is about 0.49 ± 0.04 , which is larger than that for the case of the simple strip pore. The tendency to deviate from the case of simple strip pore will be shown even clearly by enlarging R_{\max} , therefore the tilt angle θ . In Fig. 5 the pore has the same geometric parameters as that shown in Fig. 4 except R_{\max} is enlarged to $R_{\max} = 16.8\sigma$, correspondingly, $\theta = 21.8^\circ$. The configuration snapshots shown in Fig. 5 are taken at various instants after a quench at $T^* = 1.4$. As shown in Fig. 5, the plugs are formed in a narrower section of the pore. And the domain size in the wider section is larger than that in the narrower section. However, the phase separation in the wider section is still continuing until a complete phase separation in the wider section occurs at a later time, as shown in Fig. 5. It clearly demonstrates how the local pore size affects the phase separation behavior. A larger effective growth exponent of $\alpha = 0.64 \pm 0.04$ is observed at late times, as shown in Fig. 6. This value of α , characterizing the growth rate of the average size of the ordering domains in the binary fluids is close to the hydrodynamic growth exponent of $\approx \frac{2}{3}$ found in bulk two-dimensional systems [21]. We should note that one would need many ensemble realizations to establish an accurate asymptotic late-time growth exponent [22]. However, when we compare the results

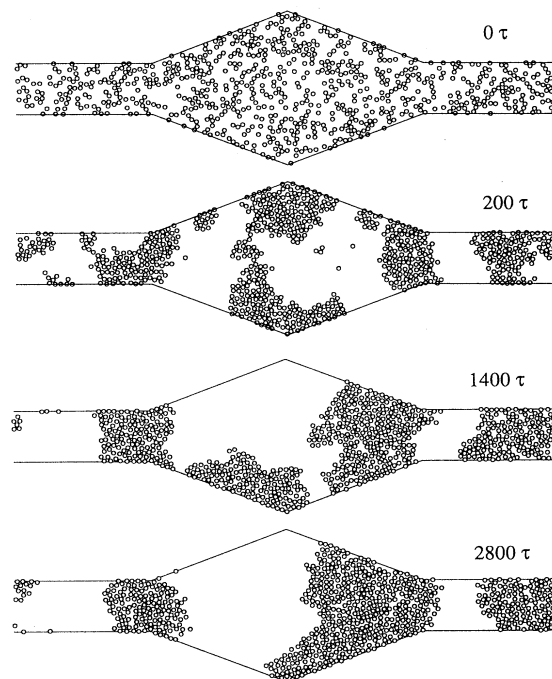


FIG. 5. The configuration snapshots of a 50-50 composition mixture confined in an uneven strip pore of $R_{\min} = 5.6\sigma$, $R_{\max} = 16.8\sigma$, and $L = 112\sigma$ at $t = 0, 200\tau, 1400\tau$, and 2800τ after a quench at $T^* = 1.4$. The reduced number density of the mixture is $\rho^* \approx 0.8$. The tilt angle in the wider section is $\theta = 21.8^\circ$. One of the two species is shown as \circ , the other one is not shown for clarity.

shown in Fig. 3 and Fig. 6, it becomes clear that for wider pores one finds a larger late-time exponent. This result clearly indicates that hydrodynamic modes become important for phase separation inside the wider section.

In Fig. 7 we show the results of a similar study of the phase separation in the presence of a pore junction. The junction is made out of two simple strip pores of $L = 84\sigma$ and $R = 5.6\sigma$. They cross and are perpendicular to each

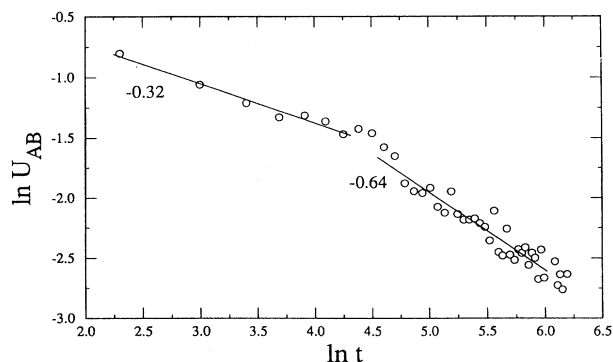


FIG. 6. Log-log plot of the repulsive potential energy between the two different species vs time for the fluid mixtures shown in Fig. 5. The solid lines with the slopes as shown are obtained as the best fits to the data, at early and late times, respectively.

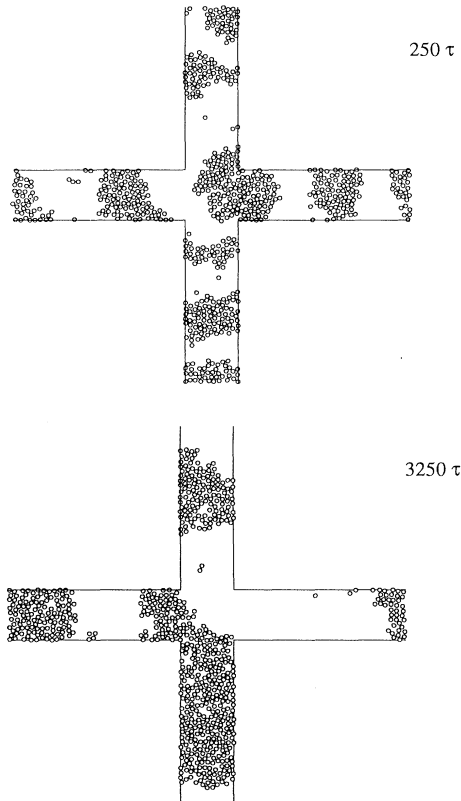


FIG. 7. Two snapshots of a 50-50 fluid mixture confined inside two crossing strip pores, at $t=250\tau$ and 3250τ after a quench at $T^*=1.4$. The reduced number density of the mixture is $\rho^*\approx 0.8$. One of the species is shown as \circ , the other one is not shown for clarity.

other. At the beginning the phase separation in the pores, shown in Fig. 7(a), is very similar to that in a simple strip pore in both the configuration pattern and the decay of the repulsive potential energies between the different species. While in the junction, domains grow faster than in the pores due to the connection to both pores. Although we do not observe a faster growth characterizing by a larger exponent in decay of repulsive potential energies, we find that the mean value of the size of the plugs in this case is much larger than that in the case of a simple strip pore, as shown in Fig. 7(b).

IV. DISCUSSIONS

In a simple strip pore, we observe a domain growth with an effective exponent of $\alpha\sim 0.3$ instead of $\alpha\sim \frac{2}{3}$ as expected for the phase separation of symmetric binary fluids in a two-dimensional bulk system. We believe that this deviation is mainly due to the confinement of the pore. The effects of the hydrodynamic mode that are present in fluids are suppressed in the narrow pore. When the pore size is increased, as in the case of the uneven strip pores, the hydrodynamic mode starts to play

a major role in the phase separation so that the effective exponent also increases. Suppression of the hydrodynamic effects has actually been observed in the phase separation in ternary-fluid mixtures [23]. It is found that a symmetric ternary-fluid system at late times reaches a dynamical scaling regime during the domains grow as $t^{1/3}$, characteristic of the long-range diffusion of molecules between the ordering domains. Although there are no physical confinements in the ternary-fluid mixtures, the strong repulsive interactions between different species and the unconnected domain-boundary network [23] may play a role similar to what the physical confinement does in a narrow pore.

One of the modifications of the present work is to check if any important modification of the single-pore model [3] is necessary for the phase separation of fluid mixtures in a true porous medium like Vycor, where there are pore junctions and variations in the pore radius. Our results indicate that the qualitative physics picture suggested by the single-pore model is still valid for more general geometries. However, the mean domain size can vary largely from position to position in porous media due to the connections of junctions and the variations in the local pore radius. It may have significant effects on the physical properties that are sensitive to fluctuations in domain size such as the intensity of light scattering [1,2].

Our results for the case of symmetric binary mixtures are consistent with those obtained in the previous molecular-dynamics simulations in three-dimensional pores [7]. On the basis of the established equivalence between the two-dimensional and the three-dimensional simulation results, we should be able to compare our data in the case of off-critical binary mixtures with recent experimental results of mixtures of PVME (poly vinyl methyl ether) and water confined in a one-dimensional capillary [5]. There is a difference in wettability to glass wall between the fluids used in the experiments. Since the difference in wettability is ignored in our simple model, we cannot compare the evolution of the pattern observed in our simulations with that of the experiment in detail. However, in deep quenches, the difference in wettability is overridden by the strong interactions between the different species. Therefore, in the case of deep quenches, our results and the experimental ones should be comparable. It seem to be the case. As shown in Fig. 4(b) in Ref. [5], in a deeper quench for off-critical PVME and water mixtures, the wetting layer becomes unstable and forms stable, periodic bridges, which is very similar to the plugs shown in Fig. 2 in this paper.

ACKNOWLEDGMENTS

This work has been supported by a grant from the National Science Foundation (DMR-9312596). The computer calculations were carried out under an NSF grant of computer time from the Pittsburgh Supercomputing Center.

- [1] See, for example, W. I. Goldberg, in *Dynamics of Ordering Processes in Condensed Matter*, edited by S. Komura and H. Furukawa (Plenum, New York, 1988).
- [2] W. I. Goldberg, F. Aliev, and X. L. Wu, *Physica (Amsterdam)* **A213**, 61 (1995).
- [3] A. J. Liu, D. J. Durian, E. Herbolzheimer, and S. A. Safran, *Phys. Rev. Lett.* **65**, 1897 (1990).
- [4] A. J. Liu and G. S. Grest, *Phys. Rev. A* **44**, R7894 (1991); L. Monette, A. J. Liu, and G. S. Grest, *Phys. Rev. A* **46**, 7664 (1992).
- [5] H. Tanaka, *Phys. Rev. Lett.* **70**, 53 (1993); **70**, 2770 (1993).
- [6] A. Bhattacharya, M. Rao, and A. Chakrabarti, *Phys. Rev. E* **49**, 524 (1994).
- [7] Z. Zhang and A. Chakrabarti, *Phys. Rev. E* **50**, R4290 (1994).
- [8] F. Brochard and P. G. de Gennes, *J. Phys. (Paris) Lett.* **44**, 785 (1983); P. G. de Gennes, *J. Phys. Chem.* **88**, 6469 (1984); D. Andelman and J. F. Joanny, in *Scaling Phenomena in Disordered Systems*, edited by R. Pynn and A. Skjeltorp (Plenum, New York, 1985).
- [9] S. B. Dierker and P. Wiltzius, *Phys. Rev. Lett.* **58**, 1865 (1987); P. Wiltzius, S. B. Dierker, and B. S. Dennis, *ibid.* **62**, 804 (1989); S. B. Dierker and P. Wiltzius, *ibid.* **66**, 1185 (1991); F. Ferri, B. J. Frisken, and D. S. Cannell, *Phys. Rev. Lett.* **67**, 3626 (1991); B. J. Frisken and D. S. Cannell, *ibid.* **69**, 632 (1992); P. Levitz and J. M. Drake, *ibid.* **58**, 686 (1987); P. Levitz, G. Ehret, S. K. Sinha, and J. M. Drake, *J. Chem. Phys.* **95**, 6151 (1991).
- [10] A. Chakrabarti, *Phys. Rev. Lett.* **69**, 1548 (1992).
- [11] D. W. Grunau, T. Lookman, S. Y. Chen, and A.S. Lapedes, *Phys. Rev. Lett.* **71**, 4198 (1993).
- [12] J. C. Lee, *Phys. Rev. Lett.* **70**, 3599 (1993).
- [13] M. P. Allen and D. J. Tildesley, *Computer Simulation of Liquids* (Clarendon, Oxford, 1989).
- [14] W.-J. Ma, A. Maritan, J. R. Banavar, and J. Koplik, *Phys. Rev. A* **45**, R5347 (1992).
- [15] P. Koblinski, W.-J. Ma, A. Maritan, J. Koplik, and J. R. Banavar, *Phys. Rev. E* **47**, R2265 (1993).
- [16] J. D. Gunton, M. San Miguel, and P. S. Sahni, in *Phase Transitions and Critical Phenomena*, edited by C. Domb and J. L. Lebowitz (Academic, New York, 1983), Vol. 8.
- [17] E. D. Siggia, *Phys. Rev. A* **20**, 595 (1979).
- [18] I. L. Lifshitz and V. V. Slyozov, *J. Phys. Chem. Solids* **19**, 35 (1962).
- [19] A. J. Bray, *Phys. Rev. Lett.* **62**, 2841 (1989).
- [20] T. Koga and K. Kawasaki, *Phys. Rev. A* **44**, R817 (1991); S. Puri and B. Dunweg, *ibid.* **45**, R6977 (1992); O. T. Valls and J. E. Farrel, *Phys. Rev. E* **47**, R36 (1993); E. Velasco and T. Toxvaerd, *Phys. Rev. Lett.* **71**, 388 (1993).
- [21] J. E. Farrel and O. T. Valls, *Phys. Rev. B* **40**, 7027 (1989).
- [22] P. Ossadnik *et al.*, *Phys. Rev. Lett.* **72**, 2498 (1994).
- [23] M. Laradji, O. G. Mouritsen, and S. Toxvaerd, *Europhys. Lett.* **28**, 157 (1994).